Biochemical and Biophysical Research Communications 462 (2015) 426–432

Contents lists available at ScienceDirect

Biochemical and Biophysical Research Communications

journal homepage: www.elsevier.com/locate/ybbrc

Alteration of cell cycle progression by Sindbis virus infection

Ruirong Yi [a], Kengo Saito [a], Naohisa Isegawa [b], Hiroshi Shirasawa [a, *]

[a] Department of Molecular Virology, Graduate School of Medicine, Chiba University Graduate School of Medicine, 1-8-1 Inohana, Chiba 260-8670, Japan
[b] Laboratory Animal Center, Graduate School of Medicine, Chiba University Graduate School of Medicine, 1-8-1 Inohana, Chiba 260-8670, Japan

ARTICLE INFO

Article history:
Received 11 April 2015
Available online 12 May 2015

Keywords:
Sindbis virus
Cell cycle
Viral replication

ABSTRACT

We examined the impact of Sindbis virus (SINV) infection on cell cycle progression in a cancer cell line, HeLa, and a non-cancerous cell line, Vero. Cell cycle analyses showed that SINV infection is able to alter the cell cycle progression in both HeLa and Vero cells, but differently, especially during the early stage of infection. SINV infection affected the expression of several cell cycle regulators (CDK4, CDK6, cyclin E, p21, cyclin A and cyclin B) in HeLa cells and caused HeLa cells to accumulate in S phase during the early stage of infection. Monitoring SINV replication in HeLa and Vero cells expressing cell cycle indicators revealed that SINV which infected HeLa cells during G_1 phase preferred to proliferate during S/G_2 phase, and the average time interval for viral replication was significantly shorter in both HeLa and Vero cells infected during G_1 phase than in cells infected during S/G_2 phase.

1. Introduction

Sindbis virus (SINV) is an RNA virus belonging to the *Alphavirus* genus in the *Togaviridae* virus family. SINV is transmitted to birds and mammals by mosquito bites and subsequently spreads throughout the body through the bloodstream [1]. SINV infection induces no or only mild symptoms (fever, rash, and arthralgia) in humans [2]. SINV has the potential to induce apoptosis in infected mammalian cells, but establishes a non-cytolytic persistent infection in arthropod cells [2,3]. In addition, the 67-kDa, high-affinity laminin receptor has been identified as a surface attachment factor that mediates SINV infection of mammalian cells [4], and is highly expressed in various human cancers [5,6].

We reported previously that SINV has oncolytic features and demonstrates antitumoral effects in various cancers, including cervical and ovarian cancer [7], and human oral squamous carcinoma cells [8]. Replication-defective SINV vectors have also been developed to target and eradicate tumors [9,10].

As an oncolytic virus, the favorable features of SINV include rapid production of high-titer virus, efficient infection of a variety of cancer cells, and a high RNA replication rate in the cytoplasm [11]. The preferable characteristics of SINV for cancer therapy might be attributed to the combination of favorable viral growth and the uncontrolled cell proliferation of cancer cells, including deregulation of the cell cycle. In normal cells, cell cycle regulator proteins, cyclin-dependent protein kinases (CDKs), cyclins, and CDK inhibitory proteins regulate progression through G_1, S, G_2 and M phases in the cell cycle. Controls by these regulators are often disturbed in cancer cells, which tend to remain in cycle [12]. Many viruses can affect the cell cycle progression of host cells to favor viral replication. Regarding DNA viruses, such as simian virus 40, adenovirus, and papillomavirus, infected cells are promoted into S phase (reviewed by Ref. [13]). Several RNA viruses also reportedly affect the cell cycle (reviewed by Ref. [14]). Recently, malignant glioma cells infected with an RNA virus, alphavirus M1, were shown to accumulate in S phase by down-regulating p21 protein [15]. The interaction between SINV replication and the host cell cycle has not been studied in detail, particularly in the context of oncolysis.

In this study, we analyzed the dynamics of cell cycle phases of HeLa and Vero cells infected with SINV in order to elucidate the interaction between SINV replication and the host cell cycle.

2. Materials and methods

2.1. Cell lines

HeLa cells were obtained from the American Type Culture Collection (ATCC; Rockville, MD). Vero cells were laboratory stock. Cells were grown in Dulbecco's modified Eagle's medium (DMEM; Sigma) with 10% fetal bovine serum (FBS) at 37 °C in 5% CO_2.

* Corresponding author. Fax: +81 43 226 2045.
E-mail address: sirasawa@faculty.chiba-u.jp (H. Shirasawa).

http://dx.doi.org/10.1016/j.bbrc.2015.04.148

2.2. Viral stocks and construction of recombinant virus

We used the laboratory stock of the AR339 strain of SINV. The plasmid pTR339-GFP-2A was kindly provided by Dr. Hans W. Heidner (University of Texas, San Antonio, TX; [16]). The BFP gene is substituted for the GFP gene in the pTR339-GFP-2A plasmid, to yield pTR339-BFP-2A.

2.3. RNA transcription

For in vitro transcription, pTR339-BFP-2A plasmid was purified using the HiSpeed Plasmid Midi Kit (Qiagen), linearized with *Xho*I (Biolab), and transcribed in vitro with the RiboMAX™ Large-Scale RNA production system-SP6 kit (Promega).

2.4. Imaging of cultured cells

Cells were grown on a 35-mm dish in DMEM with 10% FBS. After virus infection and incubation at 37 °C in 5% CO_2 for 1.5 h, cells were subjected to long-term, time-lapse imaging using a computer-assisted fluorescence microscope (Olympus, FV10i) at 37 °C in 5% CO_2. Images were recorded every 30 min. Three filter cubes were chosen for fluorescence imaging: mKusabira-orange (excitation wavelength 548 nm, emission wavelength 559 nm) to observe Fucci orange, Azami Green (excitation wavelength 493 nm, emission wavelength 505 nm) to observe Fucci green, and Blue-Narrow (excitation wavelength at 405 nm, emission wavelength 420–460 nm) to observe BFP. We used Fluoview version 3.1 (Olympus) for image acquisition and analysis.

2.5. Western blotting

Equal volumes of extracted protein were loaded onto SDS-polyacrylamide gels (Atto Corporation), transferred onto PVDF membranes (Trans-Blot Turbo™ Transfer Pack, BIO-RAD), and analyzed with antibodies.

2.6. Cell cycle analysis

Cells were collected and washed twice with PBS. Next, cells were treated with reagents from the CycleTEST™ PLUS DNA Reagent Kit (Becton Dickinson and Company) and analyzed on a BD Accuri™ C6 Flow Cytometer (Becton Dickinson and Company) equipped with FACScan's fluorescence 2 (FL2) detector. The collected data was analyzed using FlowJo 7.6.5 (TreeStar Company).

2.7. Statistical analysis

All values were expressed as mean ± SD. Statistical analyses were performed using the software Statcel2, version 2 (OMS, Tokyo, Japan). Values of $P < 0.05$ were considered statistically significant.

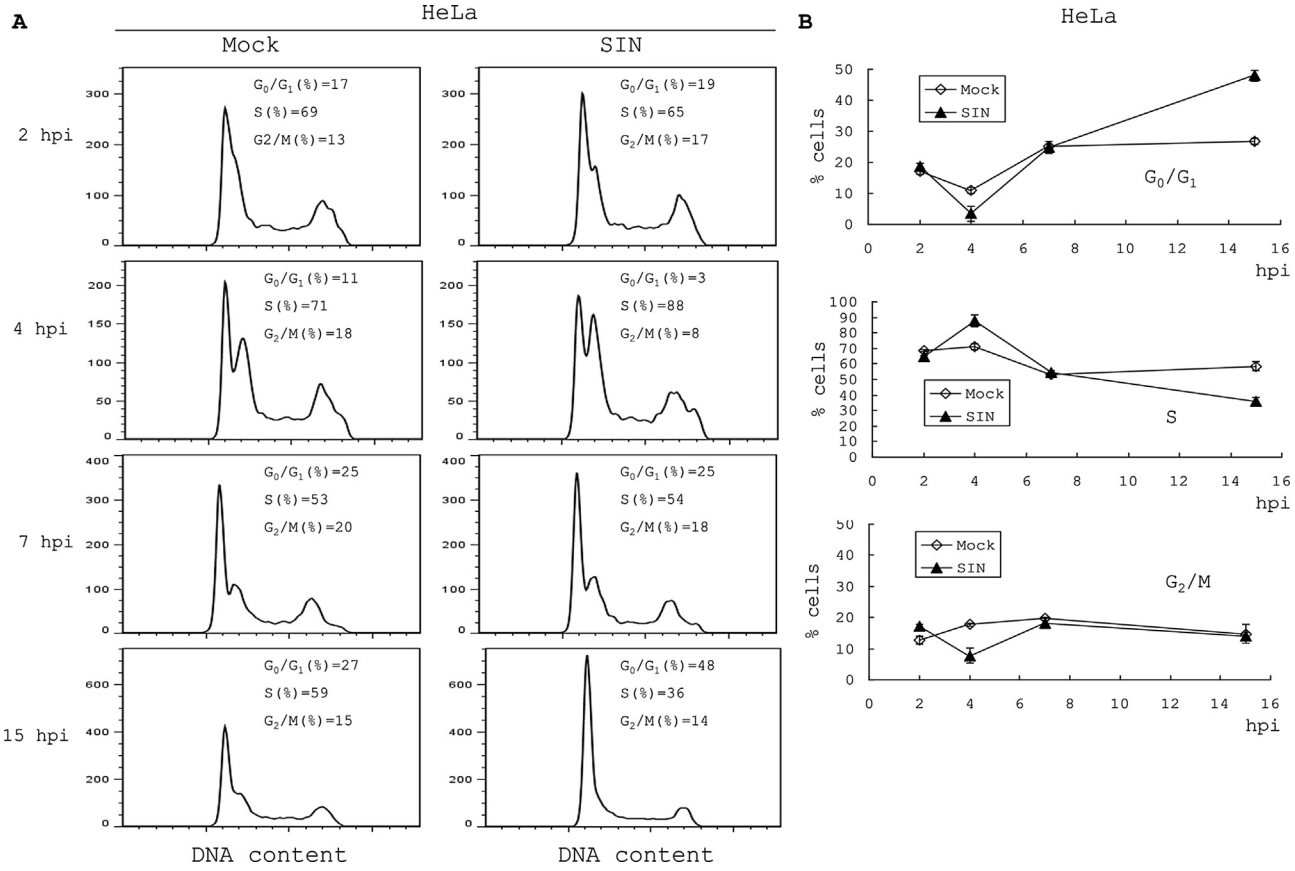

Fig. 1. The effect of SINV infection on cell cycle progression. HeLa or Vero cells were infected with 1 MOI of SINV and subjected to FACS analysis at the indicated hour post-infection (hpi). (A) FACS analysis of mock-infected (Mock) and SINV-infected (SIN) HeLa cells at 2, 4, 7, and 15 hpi. Percentages of cells in G_0/G_1, S, and G_2/M are shown. (B) The time course of proportions of mock- and SINV-infected cells in G_0/G_1, S, and G_2/M phases. (C) FACS analysis of mock-infected (Mock) and SINV-infected (SIN) Vero cells at 2, 4, 7, and 14 hpi. Percentages of cells in G_0/G_1, S, and G_2/M are shown. (D) The time course of proportions of mock- and SINV-infected Vero cells in G_0/G_1, S, and G_2/M phases. Data presented are the mean of three independent experiments. Error bars indicate standard error.

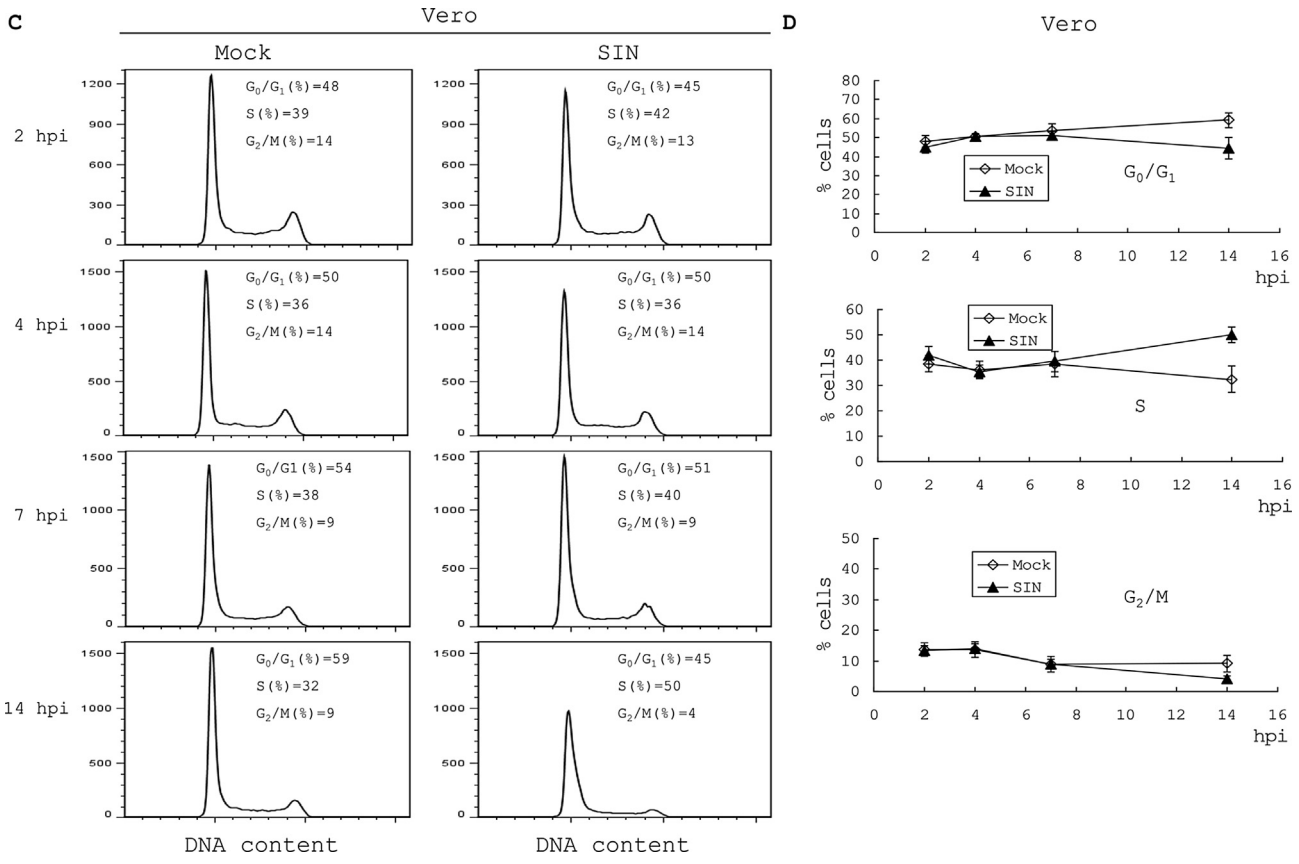

Fig. 1. (*continued*).

3. Results

3.1. Effects of SINV infection on cell cycle progression in HeLa and Vero cells

To investigate the impact of SINV infection on cell cycle progression, we used fluorescence-activated cell sorting (FACS) analysis to assess the effect of SINV infection on the distribution of HeLa and Vero cells in each phase of the cell cycle. Cells infected with 1 MOI of SINV or mock-infected were subjected to FACS analysis at 2, 4, 7, and 15 h post-infection (hpi) in HeLa cells and at 2, 4, 7, and 14 hpi in Vero cells. SINV infection significantly altered the cell cycle profile in HeLa cells (primary data are shown in Fig. 1A, and the time course of the proportion of cells in G_0/G_1, S, and G_2/M phases are shown in Fig. 1B). The proportion of HeLa cells in S phase increased and proportions of HeLa cells in G_0/G_1 and G_2/M decreased by 4 hpi, suggesting that SINV infection might simultaneously promote cell entry into S phase and prevent exit from S phase (Fig. 1A). The proportions of SINV-infected cells in each stage of the cell cycle approached the respective proportions of mock-infected cells by 7 hpi (Fig. 1B). Then, the proportions of infected cells in G_0/G_1 and S phases increased and decreased, respectively, suggesting that cell cycle progression from G_1 to S phase was blocked and that cells accumulated in G_0/G_1 at the later stage of infection.

In contrast, SINV infection caused little effect on the cell cycle progression of Vero cells during the early stage of infection (Fig. 1C). However, at the later stage of infection (by 14 hpi), the proportion of infected cells in S phase had increased and the proportions of infected cells in G_0/G_1 and G_2/M had decreased (Fig. 1D).

3.2. Effects of SINV infection on the expression of cell cycle regulators in HeLa cells

To characterize the molecular basis for the effects of SINV infection on the cell cycle in HeLa cells, we examined the levels of key cell cycle regulatory proteins. These cellular proteins were collected from mock- and SINV-infected HeLa cells at 2, 4, 7, and 15 hpi, and protein levels were measured using Western blotting (Fig. 2).

Because the cyclin D/CDK4 (CDK6) complex is active during early G_1 and regulates the progression of G_1, we examined the expression of these proteins and their regulators in infected HeLa cells. Although cyclin D1 expression was not affected by SINV infection by 7 hpi, cyclin-dependent kinases CDK4 and CDK6 were both expressed at higher levels in SINV-infected cells at 4 and 7 hpi (Fig. 2A). The elevated expression of CDK4 and CDK6 may account for the acceleration of G_1 progression, followed by the decreased proportion of G_0/G_1 cells observed by FACS analysis in HeLa cells at 4 hpi.

During late G_1, the activated cyclin E/CDK2 complex promotes the G_1/S transition by phosphorylating pRB [17]. Cyclin E, the overexpression of which shortens the duration of G_1 phase independently of pRB [18–20], increased significantly at 4 and 7 hpi in SINV-infected HeLa cells (Fig. 2B). The expression pattern of cyclin E in SINV-infected cells was similar to the expression patterns of CDK4 and CDK6. Total CDK2 expression in SINV-infected cells was not affected by the infection (Fig. 2B). Because CDK2 activity is regulated by phosphorylation at Thr160 and activated by Cdc25A-mediated dephosphorylation of Thr14 and Tyr15 [21], we examined the expression of p-CDK2 (Thr160) and Cdc25A. Although p-

CDK2 (Thr160) levels were not affected by 7 hpi, Cdc25A was expressed at a higher level in SINV-infected cells at 7 hpi (Fig. 2B). Meanwhile, the expression of p21, which binds to and inhibits the cyclin E/CDK2 complex [22,23], was decreased significantly in SINV-infected cells at 4 hpi (Fig. 2B). Taken together, the up-regulation of cyclin E and Cdc25A and down-regulation of p21 were thought to shorten G_1 and promote the G_1/S transition, in cooperation with CDK4/6-promoted G_1 progression.

Cyclin A associates with CDK2 and regulates the progression of S phase [24]. We observed suppressed cyclin A expression in SINV-infected cells at 4 hpi (Fig. 2C). This might cause retardation of S phase, and was consistent with the decrease of cells in G_2/M phase and the increase of cells in S phase in SINV-infected HeLa cells observed by FACS analysis.

Entry into M phase is signaled by the accumulation of cyclin B-cdc2, and the activation of cdc2 requires dephosphorylation at Tyr15 and Thr14 [25]. Therefore, we measured the levels of cyclin B1 and phosphorylated p-cdc2 (Tyr15) protein in SINV-infected HeLa cells. Cyclin B1 expression was suppressed in SINV-infected cells (Fig. 2C), indicating that SINV infection might block the cell cycle transition through the G_2/M checkpoint. Failure to pass the DNA replication checkpoint results in the inhibition of cdc25C activity, in turn leading to inhibition of the dephosphorylation of cdc2 [26]. Therefore, higher levels of p-cdc2 protein (the inactive form of the protein) in SINV-infected cells at 4 hpi (Fig. 2C) agreed with the temporal accumulation of cells in S phase at 4 hpi observed by FACS analysis.

At 15 hpi, the expression of cyclin D1 in infected cells was undetectable, and both CDK4 and CDK6 were expressed at low levels (Fig. 2A). The suppression of cyclin D1, CDK4, and CDK6 at 15 hpi suggested that the progression of G_1 phase should be blocked during the later stage of infection. The expression of cyclin E, p-CDK2, and Cdc25A in infected cells also decreased at 15 hpi (Fig. 2B), suggesting that the G_1/S transition should also be blocked. The suppressed expression of these proteins at 15 hpi was consistent with the increased proportion of SINV-infected HeLa cells in G_1 phase at 15 hpi observed by FACS analysis. By 15 hpi, the expression of cyclin A, which regulates the progression of S phase, had decreased in infected cells (Fig. 2C), suggesting that cells in S phase might be arrested during the later stage of infection.

3.3. Viral replication and cell cycle phases in HeLa-Fucci and Vero-Fucci cells

The differences in the cell cycle progression of HeLa and Vero cells after SINV infection might reflect differences between cancer cells and non-cancerous cells regarding the status of the cell cycle. Such differences might cause variations in viral replication depending on cell cycle phase. To test this hypothesis, we

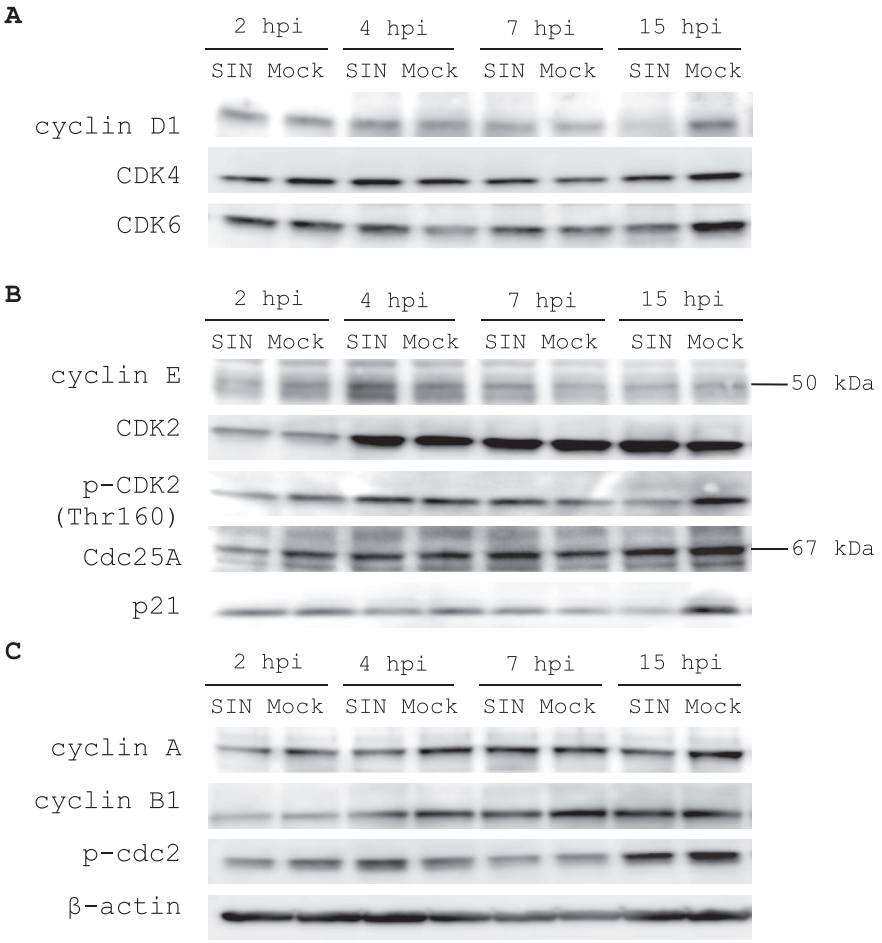

Fig. 2. Western blots of mock- and SINV-infected HeLa cells assess the expression of cell cycle regulator proteins. Total protein from SINV-infected (SIN) and mock-infected (Mock) cells at 2, 4, 7, and 15 h post-infection (hpi) were subjected to Western blotting. (A) Western blots of the G_1 phase regulators cyclin D1, CDK4, and CDK6. (B) Western blots of the G_1/S transition regulators cyclin E, CDK2, p-CDK2 (Thr160), Cdc25A, and p21. The bars indicate the positions of cyclin E and Cdc25A. (C) Western blots of cyclin A, as well as G_2/M transition regulators cyclin B1 and p-cdc2. β-actin was an internal marker for equivalent protein loading.

Table 1
HeLa-Fucci and Vero-Fucci cells infected with TR339-BFP-2A.

Cells	Cell cycle phase					
	HeLa-Fucci			Vero-Fucci		
	G_1	$S/G_2/M$	Total	G_1	$S/G_2/M$	Total
Total including uninfected at 2 hpi (%)	237(40)	362(60)	599	186(51)	178(49)	364
Infected at 2 hpi (%)	89(41)	128(59)	217	109(57)	81(43)	190
Expressing BFP						
Number of cells (%)	148(52)	134(48)	282	122(51)	116(49)	238
Number of clones (%)	89(41)	128(59)	217	90(47)	100(53)	190
Apoptosis (%)	150(53)	133(47)	283	128(53)	113(47)	241

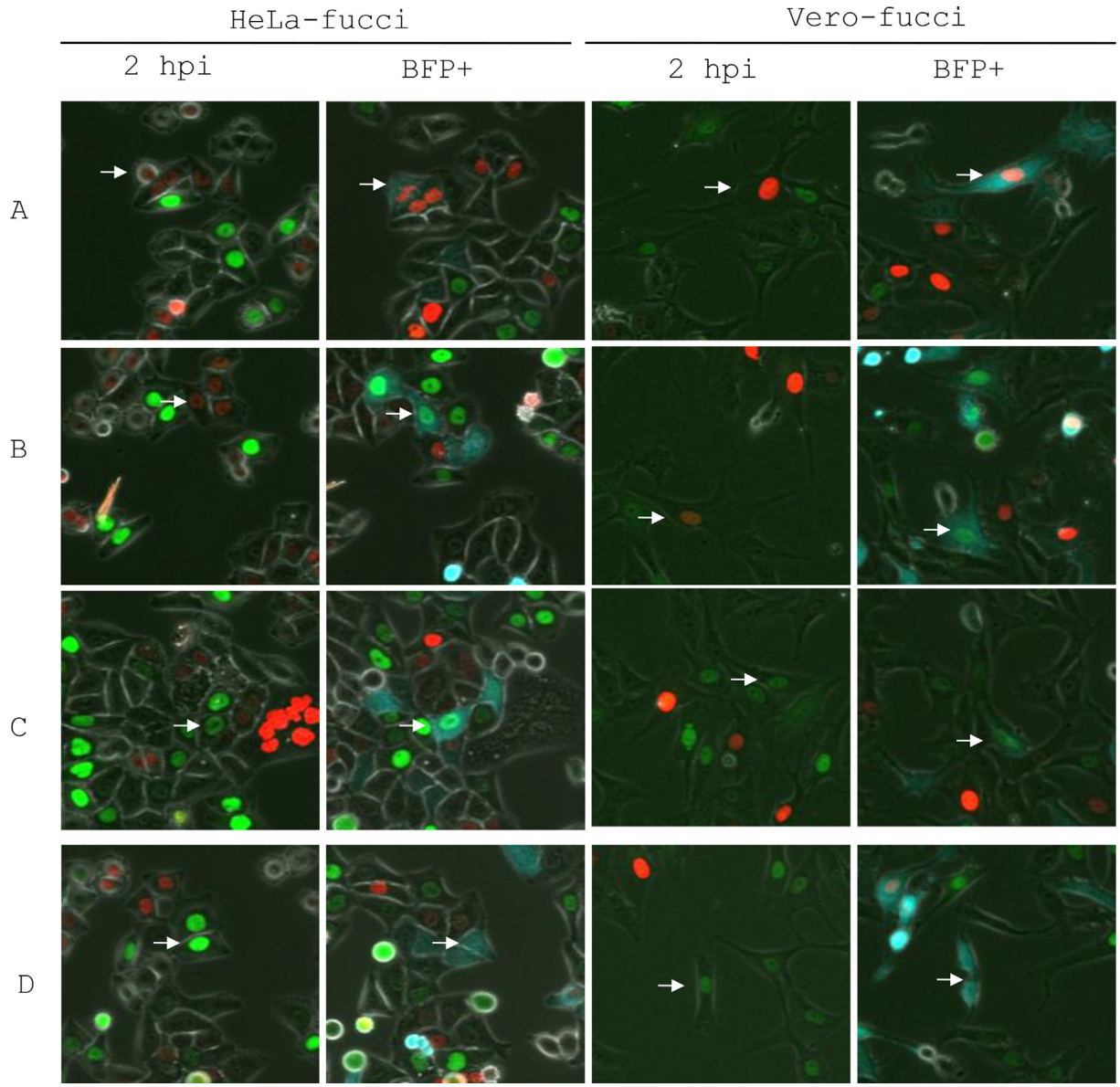

Fig. 3. The replication of BFP-expressing SINV, TR339-BFP-2A, in HeLa-Fucci and Vero-Fucci cells. Fucci labels nuclei orange during G_1 phase and green during $S/G_2/M$ phases. After infection with BFP-expressing SINV, TR339-BFP-2A, images of HeLa-Fucci and Vero-Fucci cells were obtained at 30-min intervals with a computer-assisted fluorescence microscope (Olympus, FV10i). Co-expression of blue fluorescent protein (BFP) with structural proteins from TR339-BFP-2A was observed in the cytoplasm. The lineage of each BFP-expressing cell was traced, and the cell cycle phase during which TR339-BFP-2A infection took place was determined. Arrows indicate cells that were infected during G_1 and expressed BFP during G_1 (A) or S/G_2 (B), cells that were infected during S/G_2 and expressed BFP during S/G_2 (C), or G_1 phase after cell division (D). The images shown were recorded at 2 h post-infection (2 hpi) and at the time of BFP expression (BFP+).

Table 2
Kinetics of the SINV replication in HeLa-Fucci and Vero-Fucci cells, and the cell cycle phases at infection.

Length of interval	Cell cycle phase at infection					
	HeLa-Fucci infected during			Vero-Fucci infected during		
	G_1	$S/G_2/M$	Mean	G_0/G_1	$S/G_2/M$	Mean
BFP expression (h)	9.3* (±2.0)	10.4* (±2.7)	10.0 (±2.6)	8.9† (±3.1)	10.2† (±3.4)	9.6 (±3.3)
Apoptosis (h)	13.1** (±2.4)	14.3** (±3.0)	13.8 (±2.9)	13.7†† (±3.5)	14.7†† (±3.3)	14.3 (±3.4)
Between BFP expression and apoptosis (h)	3.8 (±1.3)	3.9 (±1.4)	3.8 (±1.4)	4.9 (±1.7)	4.5 (±1.4)	4.7 (±1.5)

Standard deviations are in parentheses.
*P < 0.0001; **P < 0.005; †P < 0.005; ††P < 0.01 (all according to the Mann–Whitney U-test).

simultaneously monitored SINV replication and a cell cycle indicator, Fucci, in HeLa and Vero cells.

We established HeLa-Fucci and Vero-Fucci cell lines by introducing pFucci-G_1 orange and pFucci-$S/G_2/M$ Green-hyg (Amalgaam) successively into Vero and HeLa cells. In both cell lines, Fucci effectively labeled individual nuclei in G_1 phase as orange and those in $S/G_2/M$ phases as green [27]. To label viral replication, HeLa-Fucci and Vero-Fucci were infected with TR339-BFP-2A, which contains the BFP gene between capsid and E3, and co-expresses BFP with viral structural proteins. After viral infection with TR339-BFP-2A, HeLa-Fucci and Vero-Fucci cells were imaged using a computer-assisted fluorescence microscope (Olympus, FV10i). Images were recorded every 30 min until most cells exhibited apoptosis.

The serially collected images of 217 infected HeLa-Fucci and 190 infected Vero-Fucci cells were traced and analyzed regarding cell cycle phases, the timing of the appearance of BFP fluorescence, and the time interval between BFP appearance and apoptosis. As shown in Table 1, the proportions of infected HeLa cells in G_1 and $S/G_2/M$ phase at 2 hpi were 41% and 59%, respectively; these were equal with the proportions of total cells in G_1 (40%) and $S/G_2/M$ phase (60%), respectively. The proportions of infected Vero cells in G_1 (57%) and $S/G_2/M$ phases (43%) also exhibited no obvious difference from the proportions of total cells in G_1 (51%) and $S/G_2/M$ phase (49%), respectively.

The proportions of BFP-expressing cells in respective cell cycle phases were as follows: HeLa-Fucci, 52% in G_1 and 48% in $S/G_2/M$; Vero-Fucci, 51% in G_1 and 49% in $S/G_2/M$. When the BFP-expressing cells were traced back to 2 hpi, the respective proportions of clones in cell cycle phases G_1 and $S/G_2/M$ were 41% and 59% for HeLa-Fucci and 47% and 53% for Vero-Fucci cells. Almost all cells underwent apoptosis during the same cell cycle phase at which BFP was expressed.

Cells infected during G_1 phase expressed BFP during G_1 or S/G_2 phase, and cells infected during S/G_2 phase expressed BFP during S/G_2 or after exiting M phase (Fig. 3A–D). The mean interval between adsorption and BFP expression in cells infected during G_1 was 9.3 h for HeLa cells and 8.9 h for Vero cells. The corresponding intervals were significantly longer for HeLa-Fucci and Vero-Fucci cells infected during $S/G_2/M$ (10.4 h and 10.2 h, respectively, Mann–Whitney U-test; $P < 0.05$) (Table 2). Apoptosis was always observed a few hours after the appearance of BFP (Table 2). The mean intervals between BFP appearance and apoptosis differed between cell lines (HeLa-Fucci: 3.8 h; Vero-Fucci: 4.7 h), but did not differ significantly between cells infected during G_1 phase and those infected during $S/G_2/M$ phase (Table 2). During the interval between BFP appearance and apoptosis, the color of Fucci changed only in a few cells that expressed BFP during M phase, indicating that most cells underwent cell cycle arrest once the virus started to replicate.

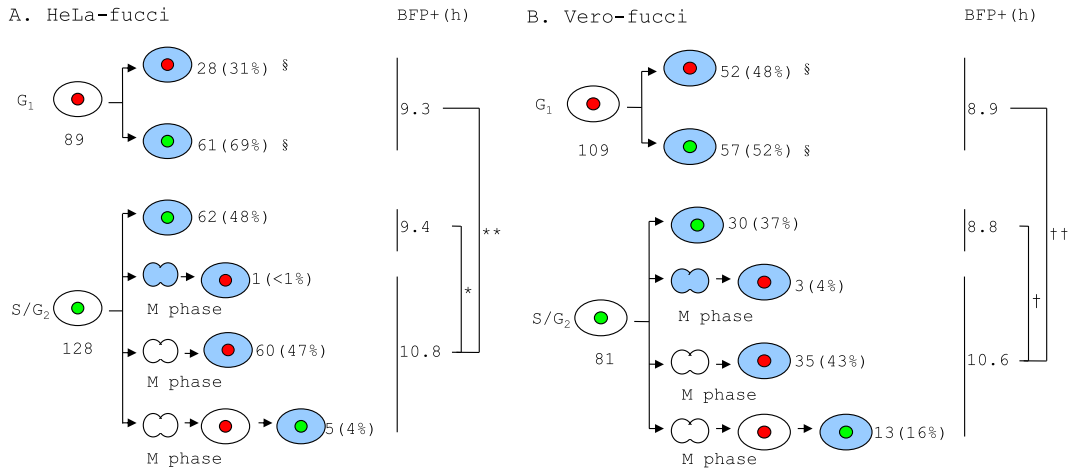

Fig. 4. Cell-cycle kinetics of HeLa-Fucci (A) and Vero-Fucci (B) cells infected with TR339-BFP-2A during G_1 and S/G_2 phase. Nuclei were labeled orange during G_1 and green during S/G_2. The lineage of each BFP-expressing cell was traced, and the cell cycle phase during which TR339-BFP-2A infection took place was determined (G_1 or S/G_2). The numbers of the traced cells are shown. The intervals between infection and BFP expression are shown at the right (BFP+). The distributions of BFP-expressing cells in G_1 and S/G_2 differed significantly between HeLa-Fucci and Vero-Fucci cells (§, P < 0.05, chi-square test). *P < 0.005; **P < 0.0001; †P < 0.005; ††P < 0.00001 (all according to the Mann–Whitney U-test).

Sixty-nine percent of HeLa-Fucci cells infected with SIN during G_1 expressed BFP after entering S/G_2; in contrast, 31% of cells infected during G_1 phase expressed BFP during G_1 phase (Fig. 4A). The preference for viral replication during S/G_2 phase in HeLa-Fucci cells was consistent with the promotion of the G_1/S phase transition by infection. Fewer Vero-Fucci cells infected during G_1 (52%) than HeLa-Fucci cells infected during G_1 expressed BFP during S/G_2 (chi-square test; $P < 0.05$) (Fig. 4B). Quite a few cells expressed BFP during M phase in both HeLa-Fucci and Vero-Fucci cells. The mean intervals between adsorption and BFP expression were significantly longer for cells that were infected during S/G_2 phase and progressed through M phase than for cells that did not progress through M phase (Mann–Whitney U-test; $P < 0.05$), suggesting that viral proliferation might be suspended during M phase.

4. Discussion

In the present study, we observed that SIN infection altered the cell cycle progression in HeLa and Vero cells; however, these cell lines' responses to SIN infection differed during the early stage of infection. SIN infection caused HeLa cells to accumulate in S phase, with the proportion of cells in G_1 and G_2/M phases decreasing by 4 hpi. Changes in the expression of cell cycle regulators during the early stage of SIN infection were considered to contribute to the promotion of the G_1/S transition and cell cycle retardation in S phase.

Using HeLa-Fucci cells infected with TR339-BFP-2A, we traced individual cells from infection to apoptosis. We confirmed that SIN, which infected HeLa cells but not Vero cells during G_1, preferred to proliferate during S/G_2, and the average length of time for viral replication was shorter in cells infected during G_1 than in cells infected during $S/G_2/M$ phase. Because cells that expressed BFP during M phase were rare in Fucci expression experiments, viral proliferation appeared to be suspended during M phase. The suspension of viral proliferation in M phase might explain why the cells that were infected during S/G_2 and progressed through M took longer to express BFP.

Given that 80–90% of cellular RNA and protein synthesis is inhibited a few hours after infection by SIN [28,29], it is noteworthy if the inhibition of RNA and protein synthesis is able to affect the expression of cell cycle regulators and cell cycle progression. In this study, after HeLa cells were infected with SIN, the expression of most cell cycle regulators exhibited no decrease at 7 hpi, but had decreased or disappeared by 15 hpi. Cell-cycle analyses between 7 and 15 hpi indicated that cell cycle progression still took place in infected HeLa cells. In experiments using Fucci-expressing cells, more than one-half of infected HeLa-Fucci and Vero-Fucci cells expressed BFP in cell cycle phases other than the phases during which infection occurred.

In conclusion, SINV infection can affect the expression of cell cycle regulators and drive cancer cells to accumulate in S phase.

Conflict of interest

None declared.

Transparency document

Transparency document related to this article can be found online at http://dx.doi.org/10.1016/j.bbrc.2015.04.148.

References

[1] D.E. Griffin, Alphaviruses, in: D.M. Knipe, P.M. Howley (Eds.), Fields Virology, fourth ed., Lippincott Williams and Wilkins, Philadelphia, 2001, pp. 917–962.
[2] J.T. Jan, D.E. Griffin, Induction of apoptosis by Sindbis virus occurs at cell entry and does not require virus replication, J. Virol. 73 (1999) 10296–10302.
[3] K. Moriishi, M. Koura, Y. Matsuura, Induction of Bad-mediated apoptosis by Sindbis virus infection: involvement of pro-survival members of the Bcl-2 family, Virology 292 (2002) 258–271.
[4] K.S. Wang, R.J. Kuhn, E.G. Strauss, S. Ou, J.H. Strauss, High-affinity laminin receptor is a receptor for Sindbis virus in mammalian cells, J. Virol. 66 (1992) 4992–5001.
[5] F.A. van den Brûle, V. Castronovo, S. Ménard, R. Giavazzi, M. Marzola, D. Belotti, G. Taraboletti, Expression of the 67 kD laminin receptor in human ovarian carcinomas as defined by a monoclonal antibody, MLuC5, Eur. J. Cancer 32 A (1996) 1598–1602.
[6] W. al-Saleh, P. Delvenne, F.A. van den Brule, S. Menard, J. Boniver, V. Castronovo, Expression of the 67 KD laminin receptor in human cervical preneoplastic and neoplastic squamous epithelial lesions: an immunohistochemical study, J. Pathol. 181 (1997) 287–293.
[7] Y. Unno, Y. Shino, F. Kondo, N. Igarashi, G. Wang, R. Shimura, T. Yamaguchi, T. Asano, H. Saisho, S. Sekiya, H. Shirasawa, Oncolytic viral therapy for cervical and ovarian cancer cells by Sindbis virus AR339 strain, Clin. Cancer Res. 11 (2005) 4553–4560.
[8] K. Saito, K. Uzawa, A. Kasamatsu, K. Shinozuka, K. Sakuma, M. Yamatoji, M. Shiiba, Y. Shino, H. Shirasawa, H. Tanzawa, Oncolytic activity of Sindbis virus in human oral squamous carcinoma cells, Br. J. Cancer 101 (2009) 684–690.
[9] J.C. Tseng, B. Levin, T. Hirano, H. Yee, C. Pampeno, D. Meruelo, In vivo antitumor activity of Sindbis viral vectors, J. Natl. Cancer Inst. 94 (2002) 1790–1802.
[10] R. Yamanaka, Alphavirus vectors for cancer gene therapy, Int. J. Oncol. 24 (2004) 919–923.
[11] K. Saito, H. Shirasawa, N. Isegawa, M. Shiiba, K. Uzawa, H. Tanzawa, Oncolytic virotherapy for oral squamous cell carcinoma using replication-competent viruses, Oral Oncol. 45 (2009) 1021–1027.
[12] C.J. Sherr, Cancer cell cycle, Science 274 (1996) 1672–1677.
[13] A. Op De Beeck, P. Caille-Fauquet, Viruses and the cell cycle, Prog. Cell. Cycle Res. 3 (1997) 1–19.
[14] S.R. Emmett, B. Dove, L. Mahoney, T. Wurm, J.A. Hiscox, The cell cycle and virus infection, Methods Mol. Biol. 296 (2005) 197–218.
[15] J. Hu, X.F. Cai, G. Yan, Alphavirus M1 induces apoptosis of malignant glioma cells via downregulation and nucleolar translocation of p21WAF1/CIP1 protein, Cell. Cycle 8 (2009) 3328–3339.
[16] J.M. Thomas, W.B. Klimstra, K.D. Ryman, H.W. Heidner, Sindbis virus vectors designed to express a foreign protein as a cleavable component of the viral structural polyprotein, J. Virol. 77 (2003) 5598–5606.
[17] R.G. Pestell, C. Albanese, A.T. Reutens, J.E. Segall, R.J. Lee, A. Arnold, The cyclins and cyclin-dependent kinase inhibitors in hormonal regulation of proliferation and differentiation, Endocr. Rev. 20 (1999) 501–534.
[18] D. Resnitzky, M. Gossen, H. Bujard, S.I. Reed, Acceleration of the G_1/S phase transition by expression of cyclins D1 and E with an inducible system, Mol. Cell. Biol. 14 (1994) 1669–1679.
[19] M. Ohtsubo, A.M. Theodoras, J. Schumacher, J.M. Roberts, M. Pagano, Human cyclin E, a nuclear protein essential for the G_1-to-S phase transition, Mol. Cell. Biol. 15 (1995) 2612–2614.
[20] J. Lukas, T. Herzinger, K. Hansen, M.C. Moroni, D. Resnitzky, K. Helin, S.I. Reed, J. Bartek, Cyclin E-induced S phase without activation of the pRb/E2F pathway, Genes. Dev. 11 (1997) 1479–1492.
[21] Y. Gu, J. Rosenblatt, D.O. Morgan, Cell cycle regulation of CDK2 activity by phosphorylation of Thr160 and Tyr15, EMBO J. 11 (1992) 3995–4005.
[22] J. Chen, P.K. Kackson, M.W. Kirschner, A. Dutta, Separate domains of p21 involved in the inhibition of Cdk kinase and PCNA, Nature 374 (1995) 386–388.
[23] F. Goubin, B. Ducommun, Identification of binding domains on p21Cip1 cyclin-dependent kinase inhibitor, Oncogene 10 (1995) 2281–2287.
[24] R.A. Woo, R.Y. Poon, Cyclin-dependent kinases and S phase control in mammalian cells, Cell. Cycle 2 (2003) 316–324.
[25] W.G. Dunphy, The decision to enter mitosis, Trends Cell. Biol. 4 (1994) 202–207.
[26] Y. Zeng, K.C. Forbes, Z. Wu, S. Moreno, S. Moreno, H. Piwnica-Worms, T. Enoch, Replication checkpoint requires phosphorylation of the phosphatase Cdc25 by Cds1 or Chk1, Nature 395 (1998) 507–510.
[27] A. Sakaue-Sawano, H. Kurokawa, T. Morimura, A. Hanyu, H. Hama, H. Osawa, S. Kashiwagi, K. Fukami, T. Miyata, H. Miyoshi, T. Imamura, M. Ogawa, H. Masai, A. Miyawaki, Visualizing spatiotemporal dynamics of multicellular cell cycle progression, Cell 132 (2008) 487–498.
[28] I. Akhrymuk, S.V. Kulemzin, E.I. Frolova, Evasion of the innate immune response: the old world alphavirus nsP2 protein induces rapid degradation of Rpb1, a catalytic subunit of RNA polymerase II, J. Virol. (2012) 7180–7191.
[29] R. Gorchakov, E. Frolova, I. Frolov, Inhibition of transcription and translation in Sindbis virus-infected cells, J. Virol. 79 (2005) 9397–9409.